FEBS 23449 FEBS Letters 470 (2000) 139–146

Structure–function relationships of the NMDA receptor antagonist peptide, conantokin-R

Tamas Blandl, Scott E. Warder, Mary Prorok, Francis J. Castellino*

Department of Chemistry and Biochemistry, University of Notre Dame, Notre Dame, IN 46556, USA

Received 21 January 2000; received in revised form 22 February 2000

Edited by Thomas L. James

Abstract Conantokin-R (con-R) is a γ-carboxyglutamate-containing 27-residue neuroactive peptide present in the venom of *Conus radiatus*, and acts as a non-competitive antagonist of the *N*-methyl-D-aspartate (NMDA) receptor. This peptide features a single disulfide bond, a type of structural element found in most classes of conotoxins, but not in other conantokins. The NMDA receptor antagonist activity of chemically synthesized con-R was determined through an assay involving inhibition of the spermine-enhanced binding of the NMDA receptor channel blocker, [^{3}H]MK-801, to rat brain membranes, and yielded an IC_{50} of 93 nM. This value represents a 2–5 times better potency than con-G or con-T, the other two characterized conantokins. Circular dichroism (CD) analysis of the metal-free form of con-R is indicative of a low α-helical content. There is an increase in α-helicity upon the addition of divalent cations, such as Ca^{2+}, Mg^{2+}, or Zn^{2+}. Isothermal titration calorimetry experiments showed one detectable Mg^{2+} binding site with a K_d of 6.5 μM, and two binding sites for Zn^{2+}, with K_d values of 150 nM and 170 μM. Residue-specific information of the conformational state of con-R was obtained by two-dimensional ^{1}H-NMR. Analyses of the α-proton chemical shifts, NOE patterns, and hydrogen exchange rates of the peptide indicated an α-helical conformation for residues 1–19. Synthetic con-R-derived peptide variants, containing deletions of 7 and 10 amino acid residues from the carboxy-terminus of the wild-type peptide, displayed unaltered cation binding and NMDA receptor antagonist properties. The α-helical secondary structures of the two truncation peptides were more stable than full-length con-R, as evidenced by CD measurements and reduced backbone hydrogen exchange rates. These results provide experimental evidence that the structural elements common to the three conantokins thus far identified are the primary determinants for receptor function and cation binding/secondary structure stability.

Key words: Conantokin-R; *N*-Methyl-D-aspartate receptor; Peptide conformation; Cation binding; γ-Carboxyglutamate

1. Introduction

Conantokin-R (con-R), a 27-residue neuroactive peptide isolated from the venom of *Conus radiatus* [1], is the third identified member of the conantokin class of neuroactive peptides, the other two peptides being con-G [2] and con-T [3]. A distinguishing feature of these biomolecules is the presence and sequence alignment of several γ-carboxyglutamic acid (Gla) residues. Aside from the several *Conus* toxins [4–6], this amino acid residue is almost exclusively found in vertebrate blood and bone proteins [7,8]. Con-R and con-T contain four Gla residues, whereas con-G possesses five such amino acids. The four Gla residues in con-T are all present in identical positions in con-G, while two of the four in con-R are in homologous locations to those in con-G and con-T. The remaining two in con-R are shifted downstream by one residue. Several other amino acids are also conserved within these peptides. These include the amino-terminal Gly–Glu sequence and an Arg preceding the Gla closest to the carboxy-terminus of the peptides. A unique feature of con-R is the carboxy-terminal extension, which contains a single five-member disulfide loop. Con-G and con-T are devoid of disulfide bonds. The majority of other conotoxins belong to one of several classes of two to four disulfide bond-containing scaffold sequence patterns [4]. The (*i*,*i*+4) spacing of the highly acidic Gla residues in these peptides allows for strong binding of divalent cations and a simultaneous adoption of a stable α-helical conformation. This phenomenon has been examined by ^{1}H-NMR structural analysis [9–13], ^{13}C-NMR [14], and by the biophysical characterization of synthetic analogues of both con-G and con-T [12,13,15,16]. There is a tight metal ion binding site formed by Gla^{10} and Gla^{14} in both con-G and con-T, while at the same time, these side chains seem dispensable for *N*-methyl-D-aspartate (NMDA) receptor antagonist activity of these peptides. On the other hand, Gla^4 and, to a lesser extent, Gla^3 were identified as crucial for the receptor inhibitory function of con-G and con-T [13,17,18].

There are indications that the conantokins have some selectivity or preference for certain subunit combinations of the NMDA receptor. In several animal models of epilepsy, con-R shows high potency and has a much better protective index for behavioral toxicity than broad-range, non-selective NMDA receptor antagonists, such as ifenprodil and MK-801 [1]. A similar argument can be made for the consideration of conantokin-based pharmaceuticals as intervention tools in several other pathophysiological processes in which the NMDA receptor has been implicated, such as stroke, Parkinson's disease, and Alzheimer's disease, among others. Therefore, closely defining the structure–function relationships of this natural antagonist will increase our understanding and

*Corresponding author. Fax: (1)-219-631 8017.
E-mail: castellino.1@nd.edu

Abbreviations: con-G, conantokin-G; con-R, conantokin-R; con-T, conantokin-T; Gla, γ-carboxyglutamic acid; NMDA, *N*-methyl-D-aspartate; DE-MALDI-TOF, delayed extraction-matrix assisted laser desorption ionization-time of flight mass spectrometry; HPLC, high performance liquid chromatography; CD, circular dichroism; ITC, isothermal titration calorimetry; NOE, nuclear Overhauser effect; NOESY, nuclear Overhauser effect spectroscopy; TOCSY, total correlation spectroscopy

PII: S0014-5793(00)01309-0

control over one of the major excitatory neurotransmitter receptor subtypes. Because of the unique structural features of con-R, the current investigation was focused on the characterization of the conformational, cation binding, and NMDA receptor antagonist properties of this newly isolated conantokin, with particular attention to the carboxy-terminal region containing the short disulfide loop.

2. Materials and methods

2.1. Peptide synthesis, purification, and characterization

Con-R (NH_2-GEγγV^{5}AKMAA^{10}γLARγ^{15}NIAKG^{20}CKVNC^{25}YP-COOH), containing a carboxy-terminal free acid group, was synthesized on a preloaded H-Pro-2-chlorotrityl resin support. The two carboxy-terminal truncation peptide amides were simultaneously synthesized on PAL resin. Reduced con-R was purified by anion exchange chromatography. A 72 h air oxidation (20°C, pH 8.5–9.0) was followed by lyophilization and desalting. The truncation variants were separated by anion exchange and desalted as described above. The peptides were characterized by reverse-phase HPLC and DE-MALDI-TOF, as described [15].

2.2. [^{3}H]MK-801 binding assays

[^{3}H]MK-801 binding assays to a brain membrane preparation enriched in the NMDA receptor were performed as previously described [13].

2.3. Circular dichroism (CD) spectroscopy

CD spectra of con-R and its analogues were collected at 25°C in 10 mM sodium borate/100 mM NaCl, pH 6.5, on an Aviv (Lakewood, NJ) model 62DS spectrometer using a 1 cm path length cell. The peptide solutions and buffers used were treated with Chelex-100 resin prior to the experiments. CD spectra of the peptides were acquired in 100% aqueous buffer with the above composition, or with the addition of 20 mM $CaCl_2$, 1.5 mM $MgCl_2$, or 1.5 mM $ZnCl_2$. The peptide concentration was 35 μM. The α-helical content was determined from mean residue ellipticities at 222 nm using the empirical relationship $f\alpha = (-[\Theta]_{222} - 2340)/30\,300$ [19].

2.4. Isothermal calorimetry (ITC)

The binding isotherms of Mg^{2+} and Zn^{2+} to the peptides were determined by ITC at 25°C in 10 mM Na–MES/100 mM NaCl, pH 6.5 buffer, as previously described [20].

2.5. ^{1}H-NMR

Peptide samples (2 mM) in a solution containing 10 mM sodium borate/100 mM NaCl, pH 6.5, 10% ^2H_2O were pre-treated with Chelex-100 resin. 2D TOCSY and NOESY spectra were collected at 5°C, using an 800 MHz Bruker-AMX or a 600 MHz Varian Unity spectrometer. The solvent H_2O signal was suppressed by transmitter presaturation or using WATERGATE [21]. Two-dimensional NMR experiments were acquired using the States–Haberkorn method for phase-sensitive detection [22] with a relaxation delay of 1.5–2 s. Mixing times were 35–75 ms (TOCSY), and 150–400 ms (NOESY). Free induction decays were acquired with 2K complex data points for the 2D data sets with a total of 280–400 t_1 increments. The NMR data were processed using VNMR (Varian), XWIN-NMR (Bruker), or the Triad module of the Sybyl software package (TRIPOS). Residue-specific assignments of the proton resonances were achieved by spin system identification from TOCSY spectra, followed by sequential assignments through NOE connectivities [23].

2.6. ^{1}H-^{2}H exchange

The 1 mM peptide samples in 10 mM sodium borate/100 mM NaCl, pH 6.5, containing 0 or 20 mM $MgCl_2$, were lyophilized, then redissolved in ^2H_2O and multiple one-dimensional proton spectra were acquired on a 500 MHz Varian Unity spectrometer as described earlier [14].

3. Results

The synthesis of linear con-R was accomplished by solid-phase methodology, followed by air oxidation to form the intramolecular disulfide bond. This peptide was purified by anion exchange chromatography, and characterized by DE-MALDI-TOF and analytical RP-HPLC. A single peptide was obtained with a molecular weight of 3099.8 (theoretical, 3100.9). The neuroactivity of synthetic con-R was established by measuring its NMDA receptor antagonist activity. For this, an assay involving inhibition of the spermine-enhanced binding of the NMDA channel blocker [^{3}H]MK-801 was used. The results of these experiments are included in Table 1, where it is observed that con-R (IC_{50} = 93 nM) is approximately 2–5-fold more potent than con-G and con-T in this assay [13,18,24].

Table 1
NMDA receptor antagonist and conformational properties of con-R and its analogues

Peptide	IC_{50} (nM)[a]	% α-helix[b]			
		apo	Ca^{2+}	Mg^{2+}	Zn^{2+}
Con-R	93	19	29	34	32
Con-R[1–20]	120	34	55	68	63
Con-R[1–17]	90	23	40	58	54

[a]Values represent the peptide concentration needed to achieve 50% inhibition of the spermine potentiation of [^{3}H]MK-801 binding to rat brain membranes.
[b]Secondary structure content of con-R analogues in the absence and presence of Ca^{2+}, Mg^{2+}, and Zn^{2+}. The % α-helix values were determined by CD measurements.

The overall conformation of the molecule was examined by CD spectroscopy (Fig. 1A). Apo-con-R has a mostly random conformation with a low (19%) α-helical content. A readily observable conformational change occurs upon the addition of the divalent cations Ca^{2+}, Mg^{2+} or Zn^{2+}. The CD changes indicate an increased α-helicity for the metal ion-bound conformations. The CD change is saturable for each metal ion (data not shown, EC_{50} values for Ca^{2+}, Mg^{2+}, and Zn^{2+} were 420 μM, 28 μM and 18 μM, respectively), also indicating a direct correlation between metal ion binding and the increase in α-helicity. The estimated α-helix contents are listed in Table 1. To further characterize the metal ion binding of con-R, ITC experiments were performed with Mg^{2+} and Zn^{2+} (Fig. 1B). A single detectable Mg^{2+} binding site was found for con-R, with a K_d of 6.5 μM. For the Zn^{2+}/con-R interaction, the best fit was provided by a two binding site model with K_d values of 150 nM and 170 μM (Table 2).

More residue-specific information regarding the conformational state of con-R was obtained by 2D ^{1}H-NMR experiments. The proton resonance assignments of con-R were completed under two solution conditions, in the absence of divalent cations and in the presence of Mg^{2+} [1] [25]. The αCH chemical shift values are compared to those for random coil values in Fig. 2. For Gla residues, the random coil value of Glu was used. In the case of apo-con-R, significant nega-

[1] Mg^{2+} was chosen as the divalent metal ion for this work since its inclusion results in a better spectral dispersion than Ca^{2+} or Zn^{2+}. Additionally, Ca^{2+} and Mg^{2+} have similar physiological concentrations, but Mg^{2+} has a higher binding affinity to con-R. Therefore, the con-R/Mg^{2+} complex is more appropriate to the biological environment. The even tighter binding cation, Zn^{2+}, is also expected to have some bound population under physiological solution concentrations. Nevertheless, Zn^{2+} was not used here because its tight binding and slow exchange lead to multiple bound conformations, which would complicate the interpretation of the ^{1}H-NMR experiments.

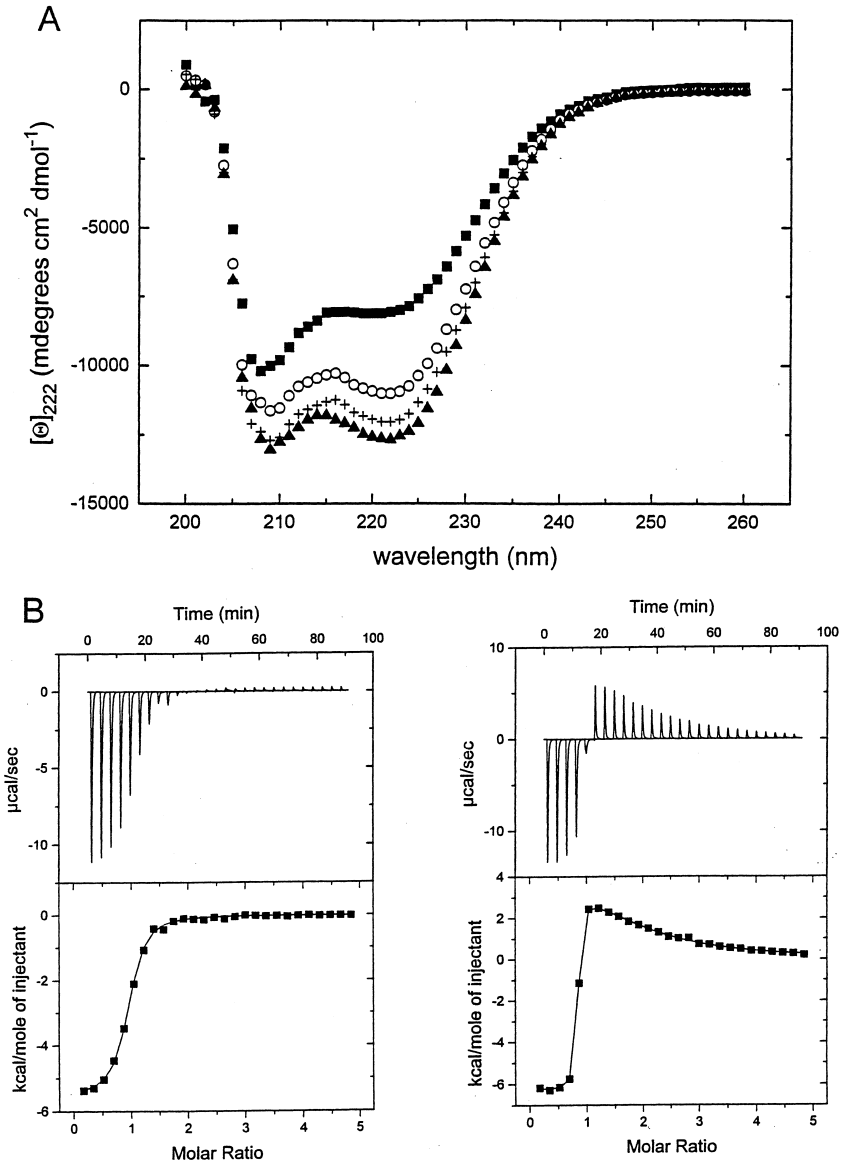

Fig. 1. Conformational and metal ion binding properties of con-R. A: CD spectra of con-R with or without multivalent cations. Spectra were recorded at 25°C in 10 mM sodium borate/100 mM NaCl, pH 6.5 using a 1 cm path length cell. The peptide concentration was 35 μM. The peptide solutions and buffers used were treated with Chelex-100 resin prior to the experiments to ensure that they did not contain multivalent cations. (■) apo-con-R; (○) 20 mM $CaCl_2$; (+) 1.5 mM $ZnCl_2$; (▲) 1.5 mM $MgCl_2$. B: Calorimetric titrations of con-R with Mg^{2+} and Zn^{2+}. The binding isotherms were determined by ITC measurements at 25°C in a buffer of 10 mM Na–MES/100 mM NaCl, pH 6.5. Peptide samples (0.4 mM) were treated with Chelex-100 resin prior to the experiments. Left panel: Mg^{2+} titration. This isotherm was fit to a one binding site model, resulting in parameters $n = 0.89$ and $K_d = 6.5$ μM. Right panel: Zn^{2+} titration. This isotherm was fit to a model describing two binding sites. The fit resulted the following parameters $n_1 = 0.77$, $K_{d1} = 0.15$ μM, $n_2 = 1.24$, $K_{d2} = 170$ μM.

tive deviations were seen for residues between Glu^2 and Lys^{19}, indicating the presence of an α-helical structure, confirming the information obtained from CD experiments. The continuity of negative chemical shift differences was interrupted at Gly^{20}, Lys^{22}, and Val^{23}, indicating that a conformation other than an α-helix characterizes the carboxy-terminal, disulfide loop-containing segment of the molecule. The α-proton chemical shift index of the Mg^{2+}-bound form of con-R, although similar to the apo form, shows several differences. The index is slightly less negative for 10 residues at the amino-terminus, perhaps indicating that the α-helical structure is less stable in this location in the presence of Mg^{2+}. The positive value for Gla^{11} in the Mg^{2+}-bound form of con-R was the only notable difference from the apo values. Similar observations were made for the equivalent residue, Gla^{10}, in both con-G [12] and con-T [13] in the presence of metal ions. This may reflect direct metal ion binding effects, and/or conformation at this residue, as was recently suggested by a structure–activity study of con-G [26]. From Leu^{12} to Ala^{18}, the chemical shift index values are comparable, or more negative than those observed for the apo form. This supports the suggestion that the strong α-helix stabilizing metal ion binding site is formed by Gla^{11} and Gla^{15}. The carboxy-terminal residues in and proximal to the disulfide loop display a chemical shift index profile similar to that of apo-con-R, with more positive values for the majority of the residues.

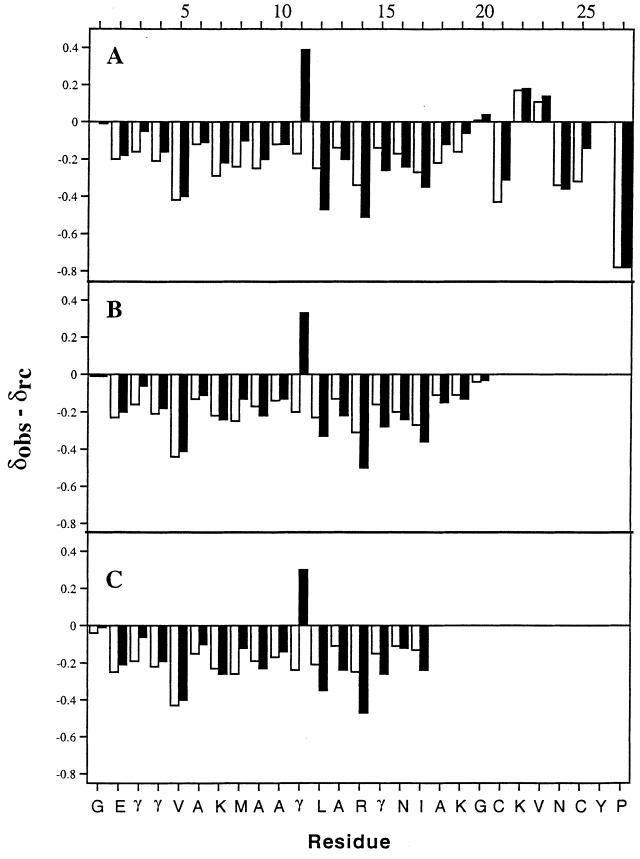

Fig. 2. Deviations of the αH chemical shifts of con-R residues from their random coil values. Gray bars, apo con-R. Black bars, con-R/Mg^{2+}. A: Con-R. B: Con-R[1–20]. C: Con-R[1–17]. The values indicated are in ppm.

The NOE patterns of apo-con-R and Mg^{2+}-con-R are illustrated in Fig. 3. The number of observed NOEs for the apo form, both sequential and medium range, is limited by persistent resonance overlap (Fig. 3A). Six (*i*,*i*+3) connections were found for the 5–16 region of the peptide, which supports the presence of a moderately stable α-helical secondary structure. Three NN(*i*,*i*+2) NOEs were also observed, which may arise from the presence of 3_{10}-helices, or from the equilibrium of random and α-helical folds. In the case of Mg^{2+}/con-R, numerous αN(*i*,*i*+3), αβ(*i*,*i*+3), αN(*i*,*i*+4) medium-range NOEs were identified for the region 2–19 (Fig. 3B). No (*i*,*i*+3) or (*i*,*i*+4) NOE cross-peaks were observed for the disulfide loop region in either form of the peptide. The sequential connectivities are absent as well for Gly^{20}–Cys^{21} and Cys^{21}–Lys^{22}.

The amide proton exchange rates in con-R were examined by NMR, in the absence and presence of Mg^{2+} ions at 5°C. Con-R in the apo state exhibited no protected proton resonances, since no amide proton signal was observed for any of the residues in this peptide after the 4 min dead time of the experiment. This indicates a $\ll 2$ min $t_{1/2}$ for every amide proton. In the presence of 20 mM Mg^{2+}, con-R showed moderate protection for four resonances (Fig. 4). Three of these correspond to Leu^{12}, Ala^{13}, and Gla^{15}. The fourth, degenerate signal was assigned to Gla^{11} and/or Arg^{14}. The $t_{1/2}$ values for each of these four resonances were estimated to be < 8 min. These moderate protection rates indicate a low secondary structural content that is marginally stabilized by hydrogen bonds. It is interesting to note that the non-exchangeable aromatic protons (at 7.15 ppm and 6.78 ppm) of Tyr^{26} are represented by two sets of resonances in a 70/30 proportion. Thus, this residue is apparently present in two distinct environments with slow exchange. In fact a second, less intensive set of resonances was found for several carboxy-terminal residues during the assignment process of con-R. The *cis-trans* isomerization of Pro^{27} may be one reason for this effect.

Two truncation variants of con-R were also synthesized and studied. In the first, seven carboxy-terminal residues were removed in con-R[1–20], eliminating the disulfide loop-containing segment of the peptide. A second peptide, con-R[1–17], possesses three fewer carboxy-terminal amino acids. This latter peptide matches the length of the shortest isolated conantokin, con-G. Both of the con-R truncation peptides were synthesized with carboxy-terminal amides. This choice was made because an amide more closely resembles the continuous peptide chain that it replaces. These two peptides were subjected to the same experiments as con-R. Table 1 includes the NMDA receptor antagonist activities of these peptides as well as a conformational analysis by CD. The NMDA inhibitory potencies of the peptides are practically unchanged, as compared to full-length con-R. There is an increased average α-helical content in both the apo and metal-bound forms of the truncated molecules. The characteristic cation-dependent increase in α-helicity is also readily observable in these truncated peptides, indicating the presence of cation binding sites. ITC experiments (Table 2) showed that each peptide has one binding site for Mg^{2+} and two different affinity binding sites for Zn^{2+}. The K_d values are similar to those of full-length con-R.

The two carboxy-terminal truncation variants of con-R were further examined by 2D ^{1}H-NMR. The ^{1}H resonance assignments of these shorter peptides were useful in the assignment process of full-length con-R. The α-proton chemical shift index pattern for these two peptides is very close for the common regions, with only slight differences (Fig. 2). Fig. 3 shows the NOE cross-peak summaries for apo and Mg^{2+}-loaded con-R truncation variants. There is a small number of (*i*,*i*+3) interactions present in apo-con-R[1–20], although

Table 2
Metal ion binding of con-R analogues as determined by ITC

Peptide	Mg^{2+}		Zn^{2+}	
	n	K_d (μM)	*n*	K_d (μM)
Con-R	0.89	6.5	0.77	0.15
			1.24	170
Con-R[1–20]	1.05	12.5	1.12	0.36
			1.04	650
Con-R[1–17]	0.98	18.0	1.01	0.19
			1.21	190

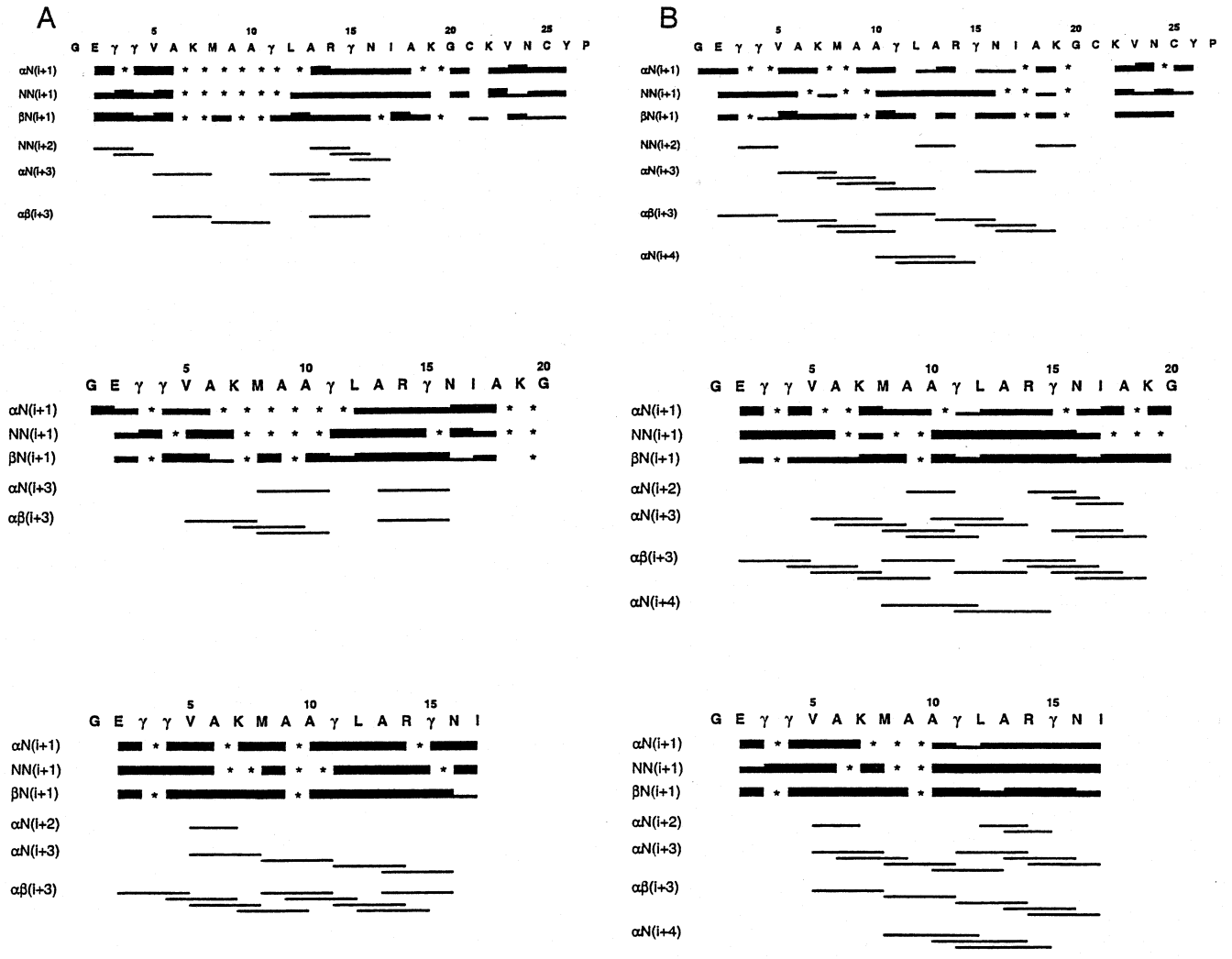

Fig. 3. Summary of the sequential and long-range NOE connectivities observed for con-R (top), con-R[1–20] (center) and con-R[1–17] (bottom) without (A) and with (B) Mg^{2+}. Line thickness correlates positively with weak, medium and strong intensity NOE cross-peaks.

degeneracy may mask some additional existing NOE connectivities. The number of observed medium-range NOE cross-peaks greatly increases in the Mg^{2+}-loaded peptide. The NN(i,i+1) NOE values are consistently strong in this peptide, also a sign of α-helical content. Similar analysis of con-R[1–17] shows (i,i+3) interactions from Glu^{2} to Asn^{16} in the apo peptide. The addition of Mg^{2+} induces several (i,i+4) NOEs, in addition to (i,i+3) backbone connectivities. All of these observations support the presence of a significant amount of α-helical secondary structure in both con-R truncation peptides.

Apo-con-R[1–20] displays more backbone proton exchange protection than either apo-con-R or Mg^{2+}-con-R, even though shorter peptide segments typically form less stable α-helices. The number of protected resonances and the extent of protection in apo-con-R[1–20] (Fig. 4) indicate the presence of significant hydrogen bond-stabilized secondary structure. Although a number of unresolved, degenerate resonances were observed in these experiments, exchangeable protons could be identified for Ala^{13}, Arg^{14}, Gla^{15}, and Asn^{16}, with HN half-lives of 180 min, 120 min, 50 min, and 12 min, respectively. The collective half-lives for the degenerate resonances at 8.20 ppm and 8.15 ppm were 100 min and 70 min, respectively. These may correspond to any or all of the Ala^{9}, Ala^{10}, Gla^{11}, Ala^{18}, and Lys^{19} (8.20 ppm) and Gla^{4}, Ala^{6}, Lys^{7}, Leu^{12}, and Gly^{20} (8.15 ppm). In the presence of Mg^{2+}, con-R[1–20] displays extensive protection from backbone proton exchange (Fig. 4). The half-lives for Ala^{13} and Gla^{15} exceed 16 h. At least one component in each of two degenerate groups, namely Gla^{4}, Lys^{7}, and Asn^{16} at 8.08 ppm, and Gla^{11}, Arg^{14}, Ile^{17}, and Lys^{19} at 7.94 ppm, possess half-lives >16 h. A backbone NH half-life of 4 h is estimated for the amide of Leu^{12}. Half-lives in the order of 4–30 min were observed for additional resonances in both apo and Mg^{2+}-loaded con-R[1–20].

4. Discussion

Con-R is a recent addition to the conantokin peptide family. This peptide shares many common features with the two more characterized members of this class of molecules, con-G and con-T, such as the tendency to adopt a helical conformation, the presence of divalent cation binding sites, and the existence of NMDA receptor antagonist activity. The three

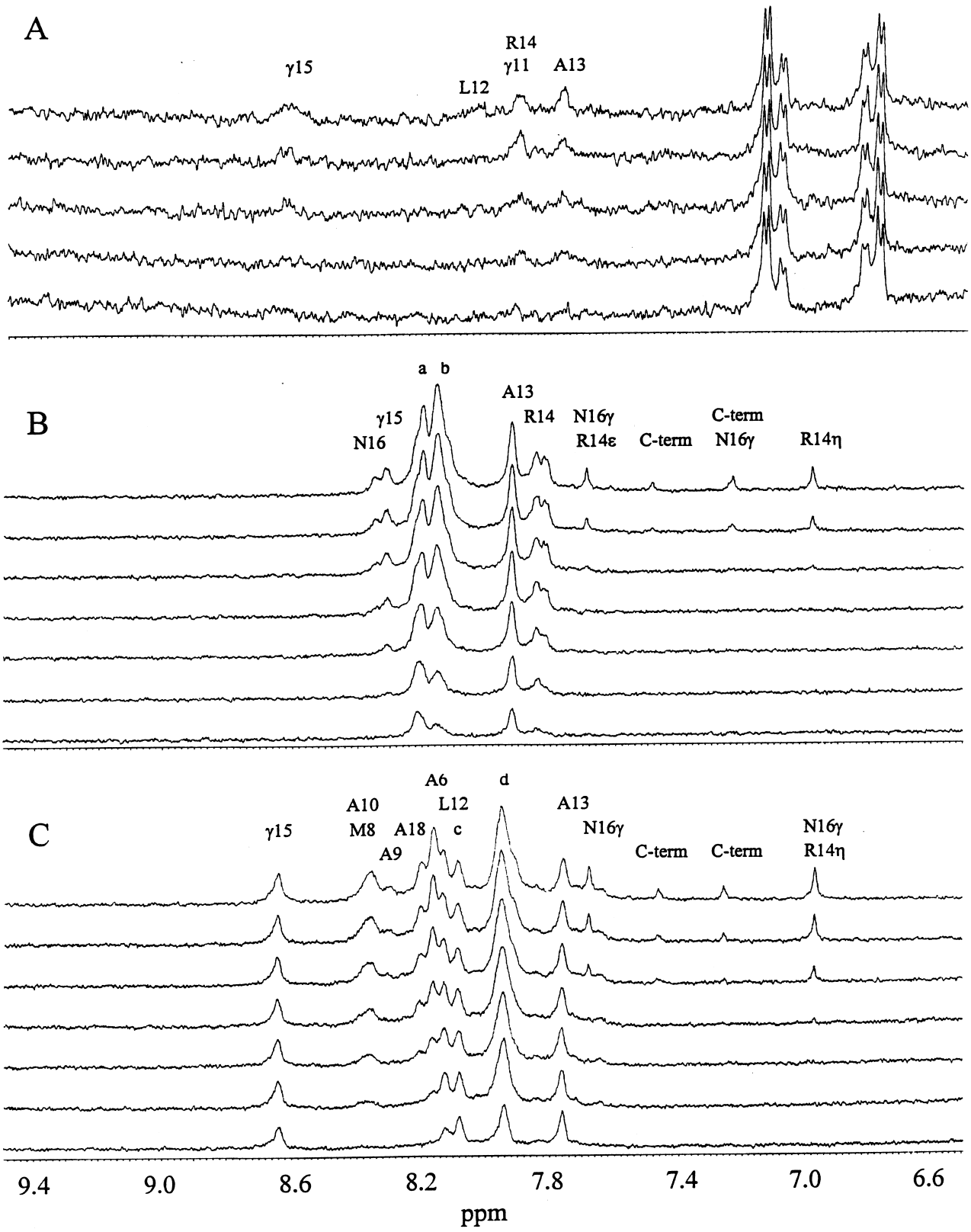

Fig. 4. Hydrogen exchange rates of con-R/Mg^{2+}, con-R[1–20] apo and con-R[1–20]/Mg^{2+} at 5°C. The amide regions of the ^{1}H-NMR spectra are shown at increasing times after dissolving the peptides in $^{2}H_2O$. Assignments of resonances are indicated above the spectra or listed below for some unresolved peaks. A: Con-R in the presence of 20 mM $MgCl_2$. Time points top to bottom: 4, 8, 16, 32 and 64 min. B: Con-R[1–20] with no Mg^{2+} present. Time points top to bottom: 4, 8, 16, 32, 64, 128, 220 min. Peak a: Ala^{9}, Ala^{10}, Gla^{11}, Ala^{18} and/or Lys^{19}. Peak b: Gla^{4}, Ala^{6}, Lys^{7}, Leu^{12} and/or Gly^{20}. C: Con-R[1–20] in the presence of 20 mM $MgCl_2$. Time points top to bottom: 4, 8, 16, 32, 64, 128 min, and 16 h. Peak c: Gla^{4}, Lys^{7}, and/or Asn^{16}. Peak d: Gla^{11}, Arg^{14}, Ile^{17} and/or Lys^{19}.

peptides have significant sequence homology, most prominently in the Gla residues. However, the amino acid sequence of con-R displays a major deviation from the primary structures of the other two related peptides, with an additional stretch of amino acids on the carboxy-terminus. This region contains a five amino acid long disulfide loop, which is a major factor in governing the solution conformation properties of con-R.

Hydrogen exchange data for full-length con-R indicate a rather unstable backbone hydrogen bonding even at 5°C. Taken together, with the α-proton chemical shift index data and the NOE patterns for the carboxy-terminal disulfide loop region, a model can be derived for the conformational behavior of con-R. The α-helix breaking effects of Gly^{20} and the disulfide bond cause an interruption in the backbone hydrogen bonding of this molecule. This counteracts the α-helix forming tendency of the preceding sequence. As a result, the amino-terminal 19 amino acids possess an only moderately stable α-helix secondary structure. Divalent metal binding, however, stabilizes the α-helical conformation. This is observable for full-length con-R, but especially evident in the case of the two amino-terminal fragments. The 10–20-fold hydrogen exchange rate difference that was observed between well resolved residues of apo and Mg^{2+}-bound con-R[1–20] represents a 0.9–1.6 kcal/mol difference in the free energy changes associated with the local unfolding of these two helical molecules [27]. While this stability difference is not large, it agrees with our other experimental results which showed that the Mg^{2+}-bound peptide has a more stable secondary structure than the apo form. The two truncation variants possess properties very much like con-G and con-T, the other two conantokins devoid of Cys loops. Extensive similarities exist between con-T and the first 20 residues of con-R. There is 50% identity between these two sequences, after accounting for the insertion at Ala^{10} in con-R. Both contain a Lys^{7} at a structurally critical position. This leads to an increased α-helical content and a reduction in the cation binding sites compared to con-G [14], which contains a Gla residue at this position.

Experimental comparison of full-length con-R with the two truncation peptides indicates that the disulfide loop near the carboxy-terminus is not essential for the NMDA receptor antagonist activity, cation binding integrity, and α-helix formation of con-R. Most other known conotoxin peptides possess two to four disulfide bridges, which impart increased structural rigidity/stability on these venom components [4,28]. The disulfide bridge in con-R perhaps serves another function, such as increased physiological half-life, in both the venom duct and the system of the prey, solubility and diffusion parameters, and/or processing subsequent to post-translational modifications. Alternatively, it may be a remnant of the evolutionary process in which strategically placed Gla residues assumed the positions of disulfide-type structural constraints in this class of *Conus* venomous peptides, perhaps functioning similarly through structural constraints imposed by cation binding.

An additional subtle structural difference between con-R and the other two conantokins is the shifted sequence positions of Gla^{11} and Gla^{15}, relative to Gla^{10} and Gla^{14} in the other two peptides. These two residues have been demonstrated to be the constituents of the primary metal ion binding site in both con-G and con-T [14]. Since their (*i*,*i*+4) spacing is maintained in con-R, it is very likely that this function is undisturbed. This is supported by the fact that the metal ion binding profile of con-R is very reminiscent of that of con-T [20]. ITC experiments revealed one Mg^{2+} and two Zn^{2+} binding sites for each molecule, with comparable affinities. A second binding site for Mg^{2+} most likely exists, but its lower affinity precludes its detection under our experimental conditions.

Binding of Zn^{2+} to each conantokin is 20–100-fold tighter than Mg^{2+} binding [20]. While there is no strict relationship of ionic radii and affinity of binding, a correlation was observed for the maximal attainable cation-induced α-helix formation – the more compact metal ions were the best α-helix inducers with con-G [16]. The ionic radii of Mg^{2+} and Zn^{2+} are comparable, thus differences in their interactions with carboxylate oxygen electron donors are the likely explanation for the observed affinity differences to the metal ion binding site formed by the Gla side chains of con-R. Zn^{2+} has filled 3d orbitals which can provide additional electrostatic interaction in complex formation. A similar observation has been made regarding the metal ion binding of a de novo designed Gla containing helix bundle peptide [29].

The physiological significance of the strong metal binding site and the α-helical conformation of the conantokin peptides is not entirely clear. Substantial carboxy-terminal truncations which eliminate the tight metal locus in both con-G and con-T are tolerated with respect to the NMDA receptor antagonist activity [18]. In addition, Ala replacements of Gla^{10} and Gla^{14} in either peptide result in only minor diminutions in bioactivity despite the observation that these alterations eliminate the primary metal ion binding site and decrease the α-helix stability. Metal ion binding and highly α-helical conformations of the conantokin sequences, like the disulfide loop segment, may provide as yet undefined advantages to the host species, other than increased receptor affinity.

In conclusion, the objectives of this study were to assess the bioactivity and conformational properties of con-R. It was found that con-R functions similarly to other members of the conantokin class of peptides. Structurally, con-R forms high-affinity multivalent cation binding sites, which stabilize and increase the subpopulation of peptide molecules containing the α-helical fold present in the apo-peptide. The short disulfide loop found on the carboxy-terminus of con-R destabilizes the α-helix. When this latter region of the peptide is removed, both divalent cation binding and NMDA receptor inhibitory properties of the peptide remain unchanged. These results provide experimental evidence that the structural elements common to the three conantokins identified thus far are the primary determinants for receptor function and cation binding/secondary structure stability.

Acknowledgements: This work was supported by Grant HL-19982 from the National Institutes of Health (to F.J.C.), the Kleiderer-Pezold family endowed professorship (to F.J.C.), a grant-in-aid from the American Heart Association (to M.P.), and a predoctoral fellowship from the American Heart Association (to T.B.).

References

[1] White, H.S., McCabe, R.Y., Armstrong, H., Donevan, S.D., Cruz, L.J., Abogadie, F.C., Torres, J., Rivier, J.E., Paarmann, I., Hollmann, M. and Olivera, B.M. (2000) J. Pharmacol. Exp. Ther. 292, 425–432.

[2] McIntosh, J., Olivera, B.M., Cruz, L. and Gray, W. (1984) J. Biol. Chem. 259, 14343–14346.
[3] Haack, J.A., Rivier, J., Parks, T.N., Mena, E.E., Cruz, L.J. and Olivera, B.M. (1990) J. Biol. Chem. 265, 6025–6029.
[4] Olivera, B.M., Rivier, J., Clark, C., Ramilo, C.A., Corpuz, G.P., Abogadie, F.C., Mena, E.E., Woodward, S.R., Hillyard, D.R. and Cruz, L.J. (1990) Science 249, 257–263.
[5] Fainzilber, M., Gordon, D., Hasson, M.E., Spira, M.E. and Zlotkin, E. (1991) Eur. J. Biochem. 202, 589–595.
[6] Fainzilber, M., Nakamura, T., Lodder, J.C., Zlotkin, E., Kits, K.S. and Burlingame, A.L. (1998) Biochemistry 37, 1470–1477.
[7] Stenflo, J., Ferlund, P., Egan, W. and Roepstorff, P. (1974) Proc. Natl. Acad. Sci. USA 71, 2730–2733.
[8] Price, P.A. and Williamson, M.K. (1985) J. Biol. Chem. 260, 14971–14975.
[9] Rigby, A.C., Baleja, J.D., Furie, B.C. and Furie, B. (1997) Biochemistry 36, 6906–6914.
[10] Skjaerbaek, N., Nielsen, K.J., Lewis, R.J., Alewood, P. and Craik, D.J. (1997) J. Biol. Chem. 272, 2291–2299.
[11] Warder, S.E., Chen, Z.G., Zhu, Y., Prorok, M., Castellino, F.J. and Ni, F. (1997) FEBS Lett. 411, 19–26.
[12] Chen, Z.G., Blandl, T., Prorok, M., Warder, S.E., Li, L.P., Zhu, Y., Pedersen, L.G., Ni, F. and Castellino, F.J. (1998) J. Biol. Chem. 273, 16248–16258.
[13] Warder, S.E., Prorok, M., Chen, Z.G., Li, L.P., Zhu, Y., Pedersen, L.G., Ni, F. and Castellino, F.J. (1998) J. Biol. Chem. 273, 7512–7522.
[14] Blandl, T., Warder, S.E., Prorok, M. and Castellino, F.J. (1999) J. Peptide Res. 53, 453–464.
[15] Prorok, M., Warder, S.E., Blandl, T. and Castellino, F.J. (1996) Biochemistry 35, 16528–16534.
[16] Blandl, T., Zajicek, J., Prorok, M. and Castellino, F.J. (1997) Biochem. J. 328, 777–783.
[17] Zhou, L.-M., Szendrei, G.I., Fossom, L.H., Maccaccheni, M.-L., Skolnick, P. and Otvos, L. (1996) J. Neurochem. 66, 620–628.
[18] Blandl, T., Prorok, M. and Castellino, F.J. (1998) FEBS Lett. 435, 257–262.
[19] Chen, Y.-H., Yang, J.T. and Martinez, H.M. (1972) Biochemistry 11, 4120–4131.
[20] Prorok, M. and Castellino, F.J. (1998) J. Biol. Chem. 273, 19573–19578.
[21] Piotto, M., Saudek, V. and Sklenar, V. (1992) J. Biomol. NMR 2, 661–665.
[22] States, D.J., Haberkorn, R.A. and Ruber, D.J. (1982) J. Magn. Reson. 48, 286–293.
[23] Wüthrich, K. (1986) NMR of Proteins and Nucleic Acids, John Wiley and Sons, New York.
[24] Zhuo, M. (1998) Eur. J. Pharmacol. 349, 211–220.
[25] Wishart, D.S., Sykes, B.D. and Richards, F.M. (1992) Biochemistry 31, 1647–1651.
[26] Nielsen, K.J., Adams, D., Thomas, L., Bond, T., Alewood, P.F., Craik, D.J. and Lewis, R.J. (1999) J. Mol. Biol. 289, 1405–1421.
[27] Mullins, L.S., Pace, C.N. and Raushel, F.M. (1997) Protein Sci. 6, 1387–1395.
[28] Myers, R.A., Cruz, L.J., Rivier, J.E. and Olivera, B.M. (1993) Chem. Rev. 93, 1923–1936.
[29] Kohn, W.D., Kay, C.M., Sykes, B.D. and Hodges, R.S. (1998) J. Am. Chem. Soc. 120, 1124–1132.